Rotation invariant color texture classification in perceptually uniform color spaces

Ramchandra Manthalkar, P. K. Biswas and B. N. Chatterji
E & ECE DEPARTMENT, Indian Institute of Technology,
Kharagpur , West Bengal, India PIN 721 302
rrm@sggs.ren.nic.in, {pkb,bnc}@ece.iitkgp.ernet.in

Abstract

$L^*a^*b^*$ **is a perceptually uniform color space and
HSV approximately perceptually uniform space for
representing color. But commonly used color space
is *RGB,* which is not perceptually uniform. In this
work we compare these three-color spaces for
rotation invariant color texture classification. The
inclusion of color aspects of texture in image
processing is increasing rapidly. Gabor wavelets are
used to obtain features. We compare the color
spaces by using two strategies. One is based on
quadratic Bayesian classifer. The other is classifier
independent based on Bhattacharyya distance
figure of merit. Perceptually uniform color spaces
gave better results.**

1. Introduction

Texture and color are two very important attributes in
image analysis. Many different methods are proposed
for texture analysis. Most of the work was focused on
gray level representation. The need to include color
aspect in texture analysis is being felt increasingly. The
important aspect of the combined problem is how
chromatic information is involved in the formation and
description of a texture. First order image properties
can be successfully determined using color
information. Texture generally describes second
(possibly third) order property of surfaces and scenes,
measured over image intensities. The use of *RGB* space
for representing image data is very general in image
processing. This is because of the availability of data
produced by the camera apparatus. *RGB* is not
perceptually uniform color space. Euclidean distances
in 3D *RGB* space do not correspond to color
differences as perceived by human beings. The
international committee on colorimetry (CIE) has
defined two color spaces, which are perceptually
uniform. These are $L^*a^*b^*$ and L*u*v*. The *L*C*H*
(Lightness, chroma, Hue) and HVC (Hue, Value,
Chroma) color apaces have been formed as derivatives
of *L*u*v* [22, 23]. Another, approximately uniform
color space is *HSV*. Main justification for using

perceptually uniform spaces is their appeal to humans
and their provision for isolating the luminance
component [22]. These are used in [12, 22, 23].
In this paper, we present a comparative study that
compares $L^*a^*b^*$ and *HSV* with *RGB* for their
effectiveness in rotation invariant color texture
analysis. A color texture is a spatio-chromatic pattern
and may be defined as the "distribution of colors over a
surface". Color aspects of textured images are studied
in [2-4, 11, 16 19-21]. It is obvious to note that
incorporating color into texture analysis is very
beneficial. Gabor filters are extensively used for
texture analysis [5,7-10,15,17]. We use a set of Gabor
filters, which extract local orientation and scale
information from different color bands. Gabor filters
are shown to be good fits for the simple cells in visual
striate cortex of human visual system. The comparison
is based on the classifier performance as well as on
classification independent measures. Classification is
based on k nearest neighbor and quadratic Bayesian
classifier. Non-classification based comparison is done
using the Bhattacharyya distance figure of merit.
Results show superior performance of perpetually
uniform spaces over RGB color space. Section 2 gives
information regarding perceptually uniform color
spaces. Section 3 introduces Gabor wavelets and
obtains the rotation invariant textures features. The
scheme to compare the performance of features in
color spaces is outlined in section 4. Section 5 gives the
experimental results. Section 6 gives the conclusion.

2. Perceptually uniform color spaces

Generally image data is given in RGB space. The
definition of $L^*a^*b^*$ is based on an intermediate
system, known as the CIE XYZ space (ITU-Rec 709).
This space is derived from RGB as given below [1]:

$$X = 0.412453R + 0.357580G + 0.180423B$$
$$Y = 0.212671R + 0.715160G + 0.072169B$$
$$Z = 0.019334R + 0.119193G + 0.950227B \quad (1)$$

$L^*a^*b^*$ color space is defined as follows [1].

$$L^* = 116 f(Y/Y_n) - 16$$

$$a^* = 500[f(X/X_n) - f(Y/Y_n)]$$

$$b^* = 200[f(Y/Y_n)] - f(Z/Z_n) \qquad (2)$$

where

$$f(q) = \begin{cases} q^{1/3} & if \quad q < 0.008856 \\ 7.87 + 16/116 & otherwise \end{cases}$$

X_n, Y_n and Z_n represent a reference white as defined by a CIE standard illuminant, D_{65} in this case. This is obtained by setting

$R = G = B = 100$ in (1), $\left(q \in \{\frac{X}{X_n}, \frac{Y}{Y_n}, \frac{Z}{Z_n}\}\right)$. HSV, is an approximately uniform color space, is defined directly on RGB. Given $R, G, B \in [0,1]$, the corresponding $H, S, V \in [0,1]$; the algorithm is given in [21].

3. Gabor wavelets

Gabor Elementary Functions are Gaussians modulated by complex sinusoids. In two dimensions they are represented by [8,15]

$$G(x, y) = G_1(x, y) \exp(2\pi j W x) \qquad (3)$$

where

$$G_1(x, y) = \left(\frac{1}{2\pi\sigma_x\sigma_y}\right)\exp\left(-\frac{1}{2}\left(\frac{x^2}{\sigma_x^2} + \frac{y^2}{\sigma_y^2}\right)\right).$$

The Fourier transform of $G(x, y)$ is

$$H(u, v) = \exp\left\{-\frac{1}{2}\left[\frac{(u-W)^2}{\sigma_u^2} + \frac{v^2}{\sigma_v^2}\right]\right\}(4)$$

where $\sigma_u = \frac{1}{2\pi\sigma_x}$ and $\sigma_v = \frac{1}{2\pi\sigma_y}$.

For localized frequency analysis it is desirable to have a Gaussian envelope whose width adjusts with the frequency of the complex sinusoids. Let $G(x, y)$ be the mother Gabor wavelet, then a filter set is obtained by appropriate dilations and rotations of mother wavelet using:

$$G_{mn}(x, y) = a^{-m}G(x', y'), a > 1, \qquad (5)$$

$$m, n = integer$$

$$x' = a^{-m}(x.\cos\theta + y.\sin\theta),$$

$$y' = a^{-m}(-x.\sin\theta + y.\cos\theta),$$

where $\theta = \frac{n\pi}{K}$ and K is the total number of orientations. The scale factor a^{-m} in equation (5) ensures that the energy is independent of scale.

$$E_{mn} = \int_{-\infty}^{\infty}\int_{-\infty}^{\infty}|G_{mn}(x, y)|^2 dx dy, \qquad (6)$$

The non-orthogonality of Gabor wavelets implies redundant information in the filtered images, and the following strategy is used to reduce this redundancy. Let U_l, U_h denote the lower and upper center frequencies of interest respectively. Let K be the number of orientations and S be the number of scales in the decomposition. Then the design strategy is to ensure that the half peak magnitude cross-sections of the filter responses in the frequency spectrum touch each other. This results in the following formulas for computing the filter parameters σ_u and σ_v (and thus σ_x and σ_y).

$$a = \left(\frac{U_h}{U_l}\right)^{\frac{1}{S-1}} \quad \sigma_u = \frac{(a-1)U_h}{(a+1)\sqrt{2\ln 2}}$$

$$\sigma_v = \tan\left(\frac{\pi}{2k}\right)\left[U_h - 2\ln 2\left(\frac{\sigma_u^2}{U_h}\right)\right].$$

$$\left[2\ln 2 - \frac{(2\ln 2)^2 \sigma_u^2}{U_h^2}\right]^{-\frac{1}{2}} \qquad (7)$$

where $W = U_h, \theta = \frac{\pi}{K} \qquad m = 0,1,...S-1$

Here m is scale. To eliminate sensitivity of the filter response to absolute intensity values, the real (even) components of the 2-D Gabor filters are biased by adding a constant to make them zero mean. Each channel is formed by a pair of real Gabor filters. Let the output of each channel is given by

$$C_{ev}(x, y; U, \theta) = G_1(x, y).\cos(2\pi U x') * i(x, y)$$

$$C_{odd}(x, y; U, \theta) = G_1(x, y).\sin(2\pi U x') * i(x, y)$$

$$(8)$$

where $G_1(x, y)$ is 2D Gaussian and $*$ denotes 2-D linear convolution.. The channel output $C(x, y)$ is computed as

$$C(x, y; U, \theta) = \sqrt{C^2_{ev} + C^2_{odd}} \qquad (9)$$

Filters are implemented in frequency domain for better computational efficiency. The mean value $M(U, \theta)$ of a channel is computed by

$$M(U, \theta) = \frac{1}{N_1 N_2}\sum C(x, y; U, \theta) \qquad (10)$$

where $N_1 N_2$ is the area of $C(x, y; U, \theta)$. This value depends on the filter center frequency U and orientation θ. The mean values provide powerful features for texture classification. These features are rotation dependant since $M(U, \theta_i) \neq M(U, \theta_j)$ for $i \neq j$. Since rotation of input image $i(x, y)$ corresponds to the translation of $M(U, \theta)$, DFT of $M(U, \theta)$ would be rotation invariant feature [9,15]. The redundant data after DFT is removed.

4. Scheme for comparing the color spaces

The rotation invariant color texture features are extracted using a set of Gabor filters. In this experimentation we have chosen 4 scales and 8 orientations. Thus the orientations are 0, 22.5°, 45°, 67.5°, 90°, 112.5°, and 135°, 157.5°. The highest spatial frequency chosen is $\dfrac{0.5}{1 + \tan(B_\theta/2)}$; here orientation bandwidth is $B_\theta = 22.5^0$. The frequency bandwidth is 1 octave. The comparison is divided in two parts. In the first part we compute the features for each texture sample. Since the aim here is to compare the effectiveness of color spaces we use Bhattacharyya figure of merit [13, 14] for a classifier independent comparison. For two classes j and k with means μ_j, μ_k and covariance matrices $\sum_j, \sum_k$, as measured in a color space, the Bhattaxharya distance of merit is defined as [14]:

$$B(j,k) = \frac{1}{8}\left(\mu_j - \mu_k\right)^T \left[\sum_j + \sum_k\right]^{-1}\left(\mu_j - \mu_k\right)$$

$$+ \frac{1}{2}\ln\left(\frac{\left|\frac{1}{2}\left(\sum_j + \sum_k\right)\right|}{\sqrt{\sum_j \sum_k}}\right) \qquad (10)$$

where $|\cdot|$ is matrix determinant. B measures pair wise separability without performing classification. The average B distance in a color space may be taken as measure of effectiveness of features for classification. In second part classification is performed based on the features. The total number of features per texture sample is 48 (i.e.16 for each color component, this is because the redundant features are not used after DFT operation). Quadratic Bayesian classifier (qbc) is used for classification. For 15-texture class k nearest neighbor classifier is also used.

5. Experimental Results

All texture images are rotated in steps of 15 degrees from 0 to 165 degrees to form the training and test images. 80 texture images from Vistex database are chosen for experimentation. For rotating the texture images "imrotate" command of Matlab is used with bicubic interpolation option and central 256×256 image is used for the experiments. An 256×256 image is divided in 16 subimages of 64×64 size, half the samples are used for training and other half for testing the performance of the classifier. The images per texture for training and test phase are 96. Table 1 gives the average Bhattacharyya distance for 15-class problem in the three color spaces. In the first experiment a subset of 15 textures is used. Table 2 gives the results of this experiment. In the second experiments the classification is done for all 80 textures using quadratic Bayesian classifier and the results are given in Table 3.

From Table 1 it is clear that the classifier independent Bhattacharya distance figure of merit is superior for perceptually uniform color spaces compared to RGB color space. The classifier results in Table 2 support the same conclusion. The performance difference between the two perceptually uniform color spaces is not very significant though the Bhattacharyya distance of merit is better for HSV compared to $L^* a^* b^*$. For the 80-texture problem, the results of which are given in table 3, the performance of perceptually uniform color spaces for classification has significant advantage over RGB color space.

6. Conclusion

A comparative experiment was designed to study the effect of different perceptually uniform color spaces for rotation invariant color texture classification. The perceptually uniform color spaces used are $L^* a^* b^*$ and HSV. Performance of these color spaces is superior to RGB color space (this is the most common color space used). We conclude from the comparison study that HVS and $L^* a^* b^*$ are better color spaces for rotation invariant color texture characterization for practical applications.

Table 1: Average Bhattacharyya distance for 15-class problem.

Color space	RGB	$L^* a^* b^*$	HSV
B average	19.85	24.7	31.38

Table 2: Percentage correct classification for 15-texture problem

Texture	RGB (knn)	RGB (qbc)	HSV (knn)	HSV (qbc)	$L^*a^*b^*$ (knn)	$L^*a^*b^*$ (qbc)
V2	97.92	95.83	91.67	95.83	98.96	97.92
V9	95.83	86.46	100	95.83	98.96	92.71
V10	72.92	75	94.79	95.83	96.88	88.54
V11	100	100	98.96	100	100	100
V27	8229	72.92	97.92	97.92	100	97.92
V32	100	100	100	100	100	100
V37	98.96	100	98.96	100	100	100
V39	97.92	98.96	100	100	100	100
V47	80.21	94.79	100	100	100	100
V52	100	100	100	100	100	100
V54	97.92	91.67	100	100	100	100
V59	97.92	100	100	100	92.71	100
V71	91.67	100	96.88	100	96.88	95.83
V75	100	96.88	100	100	97.92	97.92
V80	100	100	100	100	100	100
Overall %	94.24	94.17	98.61	99.03	98.82	98.06

Table 3: Percentage correct classification for 80-texture problem

Texture	RGB	$L^*a^*b^*$	HSV
V1	92.7083	96.875	100
V2	85.4167	100	97.9167
V3	94.7917	98.9583	100
V4	97.9167	100	100
V5	79.1667	89.5833	100
V6	79.1667	100	95.8333
V7	68.75	95.8333	98.9583
V8	96.875	100	100
V9	68.75	100	97.9167
V10	87.5	96.875	100
V11	92.7083	100	96.875
V12	97.9167	100	84.375
V13	97.9167	98.9583	98.9583
V14	85.4167	90.625	100
V15	71.875	93.75	94.7917
V16	91.6667	100	100
V17	90.625	95.8333	98.9583
V18	83.3333	90.625	96.875
V19	86.4583	87.5	100
V20	98.9583	100	100
V21	96.875	98.9583	94.7917
V22	83.3333	98.9583	96.875
V23	91.6667	97.9167	98.9583
V24	89.5833	95.8333	95.8333
V25	97.9167	97.9167	97.9167
V26	97.9167	96.875	98.9583
V27	91.6667	100	100
V28	90.625	100	100
V29	96.875	100	98.9583
V30	100	100	100
V31	86.4583	92.7083	96.875
V32	97.9167	94.7917	97.9167
V33	93.75	96.875	94.7917
V34	98.9583	100	96.875
V35	93.75	98.9583	100
V36	90.625	97.9167	100
V37	89.5833	95.8333	97.9167
V38	87.5	94.7917	91.6667
V39	90.625	93.75	100
V40	100	100	100
V41	96.875	98.9583	100
V42	92.7083	97.9167	100
V43	92.7083	100	100
V44	82.2917	100	100
V45	96.875	100	100
V46	98.9583	98.9583	92.7083
V47	98.9583	100	100
V48	82.2917	96.875	100
V49	93.75	100	96.875
V50	96.875	100	96.875
V51	72.9167	86.4583	89.5833
V52	100	100	100
V53	91.6667	92.7083	91.6667
V54	97.9167	100	100
V55	100	100	100
V56	98.9583	98.9583	100
V57	97.9167	100	100
V58	92.7083	100	98.9583
V59	95.8333	100	100
V60	93.75	94.7917	95.8333
V61	72.9167	95.8333	94.7917
V62	82.2917	98.9583	92.7083
V63	82.2917	92.7083	100
V64	77.0833	100	98.9583
V65	67.7083	100	97.9167

V66	87.5	100	100
V67	89.5833	100	100
V68	95.8333	100	100
V69	86.4583	100	96.875
V70	96.875	97.9167	100
V71	98.9583	100	100
V72	100	100	100
V73	65.625	92.7083	100
V74	96.875	100	100
V75	97.9167	100	100
V76	97.9167	98.9583	98.9583
V77	100	100	100
V78	100	100	100
V79	85.4167	98.9583	86.4583
V80	100	100	100
Overall %	**90.86**	**97.86**	**98.11**

References

[1]   Wyszecki G. W. and Stiles S. W., Color science: Concepts and methods, Quantitative Data and Formulas, New York, Wiley, 1982.

[2]   Jain A. and Healy G., "A multiscale representation including opponent color features for texture recognition," IEEE Trans. On Image Processing, vol. 7, pp. 124-128, Jan. 1998.

[3]   Paschos G., "Chromatic correlation features for texture recognition," Pattern Recognition Letters, vol. 19, pp. 643-650, 1998.

[4]   Wouwer G. V. de, Scheunders P., Livens S., Van Dyck, " Wavelet correlation signatures for color texture classification," Pattern Recognition, vol 32, pp. 443-451, 1999.

[5]   A. K. Jain, Farshid Farrokhnia, "Unsupervised texture segmentation using Gabor filters," Pattern Recognition, Vol. 4, no. 12, pp. 1167-1186, 1991.

[6]   Todd R. Reed and J. M. H. Du Buf, "A review of recent texture segmentation and feature extraction techniques," Computer Vision, Graphics, and Image Processing, Vol. 57, no. 3, pp. 359-372, 1993.

[7]   A. C. Bovik, M. Clark, W. S. Geisler, "Multichannel texture analysis using localized spatial filters," IEEE trans. On pattern analysis and machine intelligence, Vol. 21, no. 1, pp. 55-73, 1990.

[8]   George M. Haley and B. S. Manjunath, "Rotation-invariant texture classification using a complete space-frequency model," IEEE transactions on Image Processing, vol. 8, no. 2, pp. 255-269, February 1999.

[9]   T. N. Tan, "Rotation invariant texture features and their use in automatic script identification," IEEE Transactions on pattern analysis and machine intelligence, vol. 20, pp. 751-756, July 1998.

[10]   M. Porat and Y. Y. Zeevi, " The generalized scheme of image representation in biological and machine vision," IEEE Transanctions on pattern analysis and machine intelligence, vol. 36, pp. 115-129, January 1989.

[11]   Paschos G. and Valavanis K. P., "A color texture based visual monitoring system," IEEE Trans. Syst. Man, Cybern. C. vol. 29, pp. 298-307, May 1999.

[12]   Song K. Y., Kittler J. and Petrou M., "Defect detection in random color textures," Image Vision Computing, vol. 14, no. 9, pp. 667-684, 1996.

[13]   Davis L. S., M. Clearman and Aggarwal J. K., "An empirical evaluation of generalized cooccurrence matrices," IEEE Trans. On Pattern Analysis and Machine Intelligence, vol. PAMI-3, pp. 214-221, Mar. 1981.

[14]   Faugeras O., Pratt W., "Decorrelation mrthods of texture feature extraction," IEEE Trans. On Pattern Analysis and Machine Intelligence, vol. PAMI-2, pp. 323-332, July. 1980.

[15]   Ramchandra Manthalkar, P. K. Biswas, "Rotation invariant texture classification using Gabor Wavelets," Asian Conference on Computer Vision, pp. 493-498, Jan. 23-25, 2002, Melbourne Australia.

[16]   Ramchandra Manthalkar, P. K. Biswas, "Color Texture Segmentation using multichannel filtering," Conference on Digital Image Computing Techniques and Application, pp. 346-351, Jan 21-22, Melbourne, Australia, 2002.

[17]   Ramchandra Manthalkar, P. K. Biswas, B. N. Chatterji, "Rotation and scale invariant texture classification using Gabor wavelets," accepted for Second International workshop on texture analysis and synthesis 'texture 2002' to be held on June 1, 2002, Copenhagen.

[18]   Ramchandra Manthalkar and P.K. Biswas, "Rotation invariant texture classification using gabor phase features" to appear in the Special Issue of the IETE Journal of Research on Visual Media Processing, 2002.

[19]   Cheng H. D., Jiang X. H., Sun Y. and Wang Jingli, "Color inage segmentation: advances and prospects," Pattern Recognition, vol. 34, pp. 2259-2281, 2001.

[20]   Rubner Y., Puzicha J., Tomasi C. and Buhmann J. M., "Empirical evaluation of dissimilarity measures for color and texture," Computer vision and image understanding, vol. 84, pp. 25-43, 2001.

[21]   Paschos G., "Perceptually uniform color spaces for color texture analysis: an empirical evaluation," IEEE Trans. On Image Processing, vol. 10, no. 6, June 2001.

[22] Chang C. C., Wang L. L., "Color texture segmentation for clothing in a computer-aided fashion design system," Image Vision and Computing, vol. 14, no. 9, pp, 685-702, July 1988.

[23] Gong Y., Proietti G. and Faloutsos, "Image indexing and retrieval based on human perceptual color clustering," Int. Conf. On Computer vision and Pattern Recognition, June 1998.
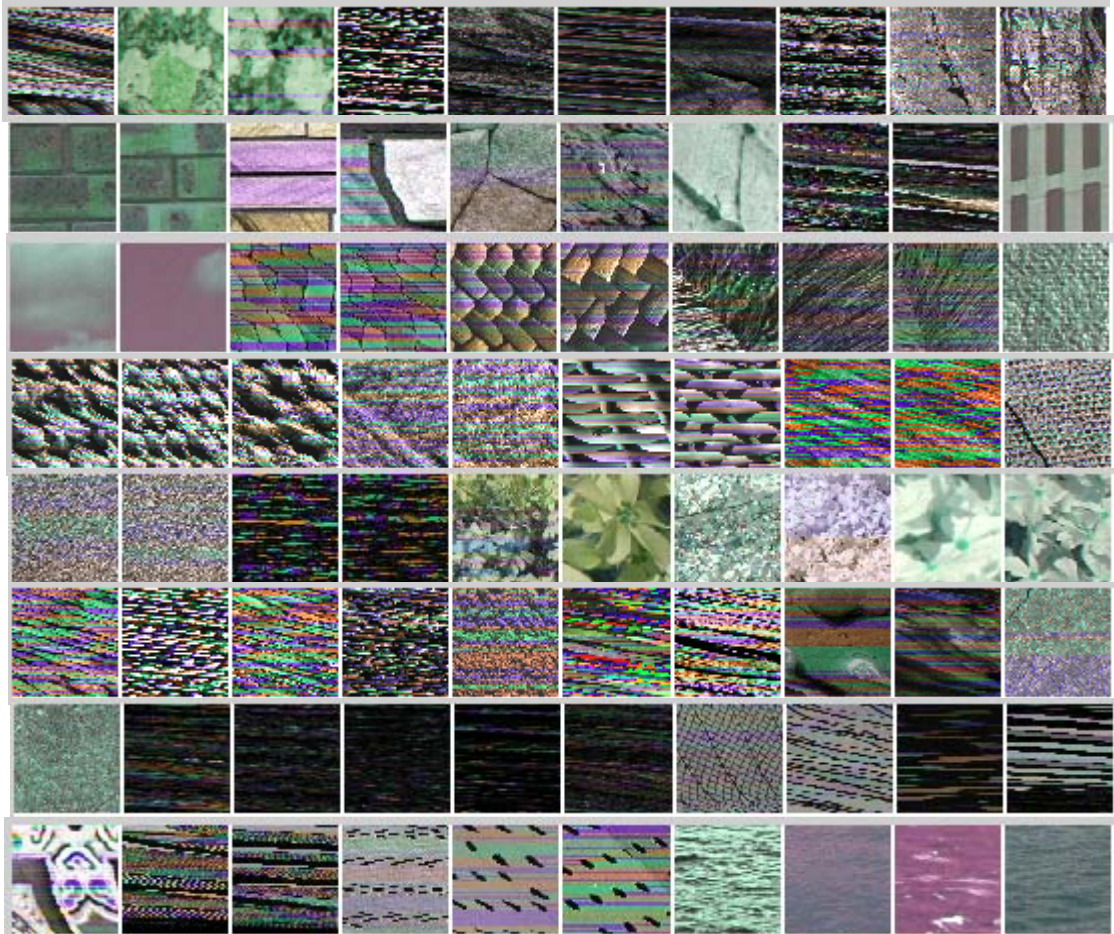
Figure 1: Textures used for rotation invariant color texture classification
Experiment from left to right and top to bottom Row1: V1=V10;
Row 2:V11-V20; Row 3: V21-V30; Row 4: V31-V40; Row 5: V41-V50;
Row 6:V51-V60; Row 7: V61-V70; Row 8 V71-V80.